International Journal of Applied Engineering Research ISSN 0973-4562, Volume 14, Number 7 (2019) pp. 1584-1592

Power Transformer Hot Spot Temperatures Estimation based on Multi-attributes

Edwell. T. Mharakurwa
Electrical Engineering
Pan African University Institute for Basic Sciences, Technology and Innovation (PAUSTI),
P.O. Box 62000-00200, City Square
Nairobi, Kenya

George. N. Nyakoe
Electrical Engineering
Jomo Kenyatta University of Agriculture and Technology (JKUAT)
P.O. Box 62000-00200, City Square,
Nairobi, Kenya

A. O. Akumu
Electrical Engineering
Tshwane University of Technology (TUT)
Private Bag X680 0001,
Pretoria, South Africa

Abstract
Operational thermal stresses due to dynamic loading and changing environmental conditions enhance the weakening of the power transformer insulation system. During the operation of power transformers, insulation hot spot temperature is a critical parameter that needs to be held under recommended threshold. This is because, amid other factors, cumulative effect of insulation aging depends on time change of hot spot temperatures. In this paper, a multi-parameter based thermal model established upon a thermal-electric circuit scheme to estimate transformer hot spot temperatures is proposed. The model includes the effects of solar irradiation, varying ambient temperatures, dynamic loading and the nonlinear thermal resistance of oil-paper insulation. Moisture effect is considered in estimating the thermal resistance of cellulose, whilst in calculation of oil insulation nonlinear thermal resistance, a universal thermal model is proposed which uses some transformer design-dependent variables and considers different heat transfer modes inside a transformer. The multi-parameter model is validated using data collected from in-service mineral oil immersed transformers. Simulated results of the proposed thermal model are in agreement with the on-site measured values with good model accuracy.

Keywords: dynamic loading, hot spot temperatures, thermal resistance, thermal stress

1. INTRODUCTION

Power transformation is the integral part of any grid system; hence a power transformer is a critical component for any power delivery system. A transformer subjected to electrical, thermal, mechanical and chemical stresses, is prone to failure due to faults thereby causing extensive financial losses to the utility and undesirably affecting the system reliability. Due to thermal inhomogeneity of transformer windings, transformers can experience undesirable temperature rise. In addition, localized temperature rise in windings increment is by dynamic load currents thereby leading to hot spot temperatures (HST). These HST and top oil temperature (TOT) can cause accelerated thermal degradation of insulation and successive thermal run away if limiting thresholds are surpassed. Therefore, it is of great importance to estimate the HST and TOT accurately to avoid catastrophic failure of power transformers.

In [1]-[3], it is suggested that the hot spot temperatures and the performance of the cooling system are essential restrictive factors for loading of power transformers. Insulation exposed to high regions of HST has an accelerated rate of degrading due to high thermal stress. This reduces the technical lifespan of the transformer [4]. In addition, HST precise estimation improves power reliability since it is an essential factor governing transformer operation efficiency and life expectancy. Therefore, it is vital to determine the HST under dynamic loading and varying environmental conditions.

Optic fiber sensor technique, recommended as the best direct method to measure HST proved to be very expensive and impractical for aged transformers to install sensors inside the winding without disturbing the performance of the transformer [5]. This has led to continued use of winding temperature indicators (WTI) as hot spot temperature measurement technique in aged and some new transformers. Accordingly, many thermal models for TOT and HST has evolved as suggested in literature but not limited to IEEE [1], IEC [2], convectional thermal-electric based models [6]-[11], Moisture-Dependent Thermal Model [12] and artificial intelligent based models [13]-[14]. In [10]-[11], emphasis was on improving the top oil temperature estimation under dynamic loading. However, most of these existing thermal dynamic models obtain inconsistent results when applied to different transformers conditions because many assumptions are made during model formulation.

Un-involvement of the effect of solar radiation in conventional models has led to underestimates in TOT and HST calculations. Cui et al., [12], also noted that existing models only consider the thermal resistance of the oil in the hot spot calculations of the transformer. However, both temperature and moisture affect the thermal properties of the cellulosic insulation. In addition, the calculated thermal resistance is estimated to be constant. This has led to overestimates in HST calculations. Therefore, it is necessary to take the varying thermal resistance of both oil and cellulose into account in a transformer with different heat transfer modes when determining transformer top oil and hot spot temperatures.

2. THERMAL MODELING

Modeling of the heat transfer phenomena in an operating transformer is a complicated task especially when the transformer is subject to simultaneous acting of different stress levels. Common models used for TOT and HST calculations emanated from [1], [2] for oil immersed transformers, where it is assumed that TOT inside and along the windings increases linearly from

bottom to top. In developing thermal models, thermal resistance of a transformer is also of major concern where most models consider it constant. Thus, the model proposed in this paper also improves the accuracy of the thermal model by considering varying heat transfer modes that affects the thermal resistance of the transformer.

2.1 Top Oil Thermal Model

The top oil temperature model calculations centers on a thermal circuit developed from a thermal-electrical analogy and heat transfer theory [6]. Without considering the solar irradiation effect and moisture effect in insulation thermal resistance, the top oil temperature of the transformer is calculated using equation (1):

$$\left[\frac{K^2.R+1}{R+1}\right].\Delta\theta_{o,R}^{\frac{1}{n}} = \tau_{o,R}\frac{d\theta_o}{dt} + (\theta_o - \theta_a)^{\frac{1}{n}} \quad (1)$$

where, $\Delta\theta_{o,R}$ is rated top oil temperature rise above ambient, θ_o represents top oil temperature, θ_a is ambient temperature, $\tau_{o,R}$ denotes rated oil time constant, R shows the ratio between transformer load loss and loss of transformer during no load tests, K denotes ratio between load current and rated winding current, n is a constant signifying nonlinearity in top oil thermal model for different cooling modes.

Gorgan et al, [15] noted that solar irradiation could alter the top oil temperature rise especially in areas where transformers are exposed to high varying ambient temperatures. Equation (1) is modified to take into account the effect of solar irradiation and effect of moisture in insulation thermal resistance. In addition, the thermal resistance of oil calculations is done by considering different heat transfer modes inside the transformer. The thermal-electrical circuit for TOT model showing the heat transfer modes inside the transformer is shown in Fig. 1. There are three current sources used to represent the heat sources of; no load loss (q_{Fe}), load loss of transformer (q_{Cu}) and effect of solar irradiation (q_{Rad}) (external heating) on outdoor transformers. In this paper, solar radiation is taken as heat source as it causes top oil temperature rise, thus having an impact in transformer top oil temperature variability and indirectly heating the active parts of the transformer. The nonlinear thermal resistance consists of thermal conduction resistance of cellulose (R_{cel}) and of the convection resistance of transformer oil (R_{oil}). In addition, the lumped thermal capacitance consists of cellulose (C_{cel}) and oil (C_{oil}).

The differential equation formulated from Fig. 1 to calculate the top oil temperature is expressed as:

$$q_{Fe} + q_{Cu} + q_{Rad} = (C_{cel} + C_{oil})\frac{d\theta_o}{dt} + \frac{\theta_o - \theta_a}{R_{oil}+R_{cel}} \quad (2)$$

A factor of heat loss due to solar irradiation is considered in equation (2). Solar irradiation received at the transformer surface is a variable parameter. The total heat flux due to solar radiation calculation depend on the radiation angle (α) of the sun with respect to the surface area, ground reflection factor (ρ), weather conditions such as cloud cover, precipitation percentage and fog and also shadows casted by nearby structures. The calculated heat flux used in this paper depends on the amount of irradiation, proportional with the effective top side area and cooling capability of the transformer. The equations in [16] were used to calculate the heat flux as a function of latitude and time of day and year.

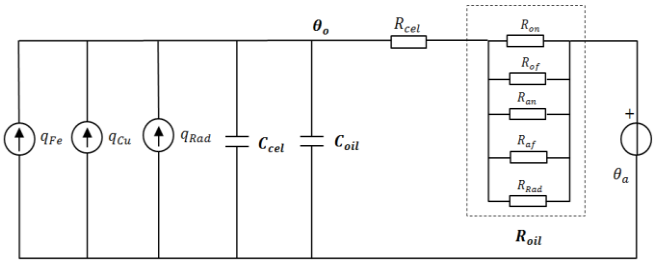

Fig. 1: Top oil temperature thermal circuit.

2.1.1. Modeling of insulation oil thermal resistance

The calculation of thermal resistance of mineral-oil insulation centers on modeling of different heat transfer ways inside the transformer. A mineral oil-immersed transformer with two coolants for heat dissipation is considered in this study. The two coolants are oil in the tank and cooler as well as air outside of the cooler. The leading equations of the oil and the air side in the modeling procedure are calculated separately with consideration of their conjoint impacts. All the thermal resistances proposed in this model depend on the thermal properties of the mineral oil and the air, whose values are also temperature dependent.

(a) Mineral Oil Equations

Oil side equations consist of two parts namely thermal resistance due to natural oil convection (R_{on}) and contribution of pumps representing forced convection (R_{of}) assuming that there is uniform flow and mixing of oil. In [8], the thermal resistance of oil due to natural convection is given as:

$$R_{on} = \frac{\mu^n}{A_o.C_1\Delta\theta_o^n} \quad (3)$$

where, μ is the oil viscosity, n is a constant representing nonlinearity in top-oil thermal model for different cooling modes, A_o denotes the surface of heat transfer (m^2) of the oil (design-dependent parameter area), C_1 is a constant as formulated in [8]. The viscosity dependence on temperature is given by the following expression, [8, 12]:

$$\mu = 1.36 \times 10^{-6} e^{\frac{2797.2}{\theta_o+273}} \quad (4)$$

In [17, 18], the thermal resistance of the forced convection of the oil due to influence of pumps is calculated as follows:

$$R_{of} = \frac{1}{h_f.A_o} \quad (5)$$

where h_f is the heat transfer coefficient ($W/(m^2.K)$) by oil forced convection defined as:

$$h_f = \frac{k_o}{l_o}.C_o(Re_o^{m'} \times Pr_o^{n'}) \quad (6)$$

where C_o , m' and n' are empirical factors depending on laminar/turbulent flow of oil , k_o denotes the thermal conductivity of oil, l_o represents the characteristic length of the system, Pr_o is Prandtle number on the oil side [8, 17,18] and Re_o is the Reynolds number defined as in equation (7):

$$Re_o = \frac{V_{m,o}.d_o}{v_o} \tag{7}$$

where, $V_{m,o}$ represents the average oil velocity assumed to be proportional to the number of switched on pumps, d_o denotes the characteristic diameter of the oil duct (design dependent factor) and v_o is the oil kinematic viscosity. The thermal resistance equivalent to forced convection of the oil due to the operation of pumps is:

$$R_{of} = \frac{l_o}{A_o C_o (Re_o^{m'} \times Pr_o^{n'})\, k_o} \tag{8}$$

(b) Air side equations

The air-side equations comprise of three thermal resistances: natural convection, radiation, and forced convection due to operation of fans.

(i). Resistance due to Forced convection

In [17], [18], the thermal resistance of the forced convection due to influence of running fans is calculated as follows:

$$R_{of} = \frac{1}{\gamma_f . A_a} \tag{9}$$

where, γ_f is the heat transfer coefficient by air forced convection defined as:

$$\gamma_f = \frac{k_a}{l_a}. C_a (Re_a^{m''} \times Pr_a^{n''}) \tag{10}$$

where C_a , m'' and n'' are empirical factors, k_a denotes the thermal conductivity of air, l_a represents the characteristic length of the heat transfer (m), $A_a$denotes the surface of heat transfer (m^2) of the air (design-dependent parameter), Pr_a is Prandtle number on the air-side [8], [17], [18] and Re_a is the Reynolds number defined as:

$$Re_a = \frac{V_{m,a}.d_a}{v_a} \tag{11}$$

where, $V_{m,a}$ represents the average air velocity assumed to be proportional to the number of operating fans, d_a denotes the characteristic diameter of the air side (design dependent) and v_a is the air kinematic viscosity.

The thermal resistance equivalent due to forced convection of the air due to the operation of fans is given by:

$$R_{af} = \frac{l_a}{A_a C_a (Re_a^{m''} \times Pr_a^{n''})\, k_a} \tag{12}$$

(ii). Resistance due to Radiation

According to Stefan-Boltzmann law, the thermal conductance of radiation is described as follows:

$$\Lambda_{rad} = \sigma \varepsilon A_{rad} (\theta_{o-a}^4 - \theta_a^4) \tag{13}$$

where, σ is the Stefan-Boltzmann constant, ε is emissivity, A_{rad} is the effective surface of radiation (design dependent) and θ_{o-a} is the logarithmic average temperature of the oil and the air, θ_a is ambient temperature.
Therefore, the resistance due to radiation (external heat dissipation) is given by the following expression:

$$R_{rad} = \frac{1}{\Lambda_{rad}} \tag{14}$$

(iii). Resistance due to Natural Convection

The thermal resistance of air for natural convection of air expressed in [8] is:

$$R_{an} = \frac{l}{A_a C [Gr \times Pr]^x k} \tag{15}$$

where, *C* and *x* are experimental constants dependent on whether the air circulation is laminar or turbulent, Gr is Grashof number [8], [17], [18], k is air thermal conductivity and *l* represents characteristic length of the heat transfer (m).
The overall convection resistance of transformer oil is expressed as in equations (16) - (18):

$$R_{oil} = R_{on} + R_{of} + R_{an} + R_{af} + R_{rad} \tag{16}$$

$$R_{oil} = \left[\frac{\mu^n}{A_o . C_1 \Delta\theta_o^n} + \frac{l_o}{A_o C_o (Re_o^{m'} \times Pr_o^{n'})\, k_o} + \frac{l}{A_a C [Gr \times Pr]^x k} + \frac{l_a}{A_a C_a (Re_a^{m''} \times Pr_a^{n''})\, k_a} + \frac{1}{\Lambda_{rad}}\right] \tag{17}$$

$$R_{oil} = \frac{\mu^n}{A_o . C_1 \Delta\theta_o^n} + \nu \tag{18}$$

where,

$$\nu = \left[\frac{l_o}{A_o C_o (Re_o^{m'} \times Pr_o^{n'})\, k_o} + \frac{l}{A_a C [Gr \times Pr]^x k} + \frac{l_a}{A_a C_a (Re_a^{m''} \times Pr_a^{n''})\, k_a} + \frac{1}{\Lambda_{rad}}\right]$$

The calculated thermal resistance for oil insulation (17) is a universal model that can be easily implemented for all transformer-cooling modes. Thus, the parameter v caters for other transformer cooling modes other than ONAN.

2.1.2 Modeling of Cellulose Thermal Resistance

Due to moisture ingress from the environment and cellulose degradation, moisture can exist in an in-transformer. Since oil has low moisture affinity, most moisture is associated with its cellulose insulation during normal transformer operation. Moisture manifest in cellulose insulation in any of the three states: adsorbed to the cellulose surface, as free water attached on capillaries, or as imbibed free water [19], [20]. A commonly used method to determine the water content of paper (WCP) is to measure the temperature and vapour

pressure of water of the oil. In this paper, online capacitive probes to measure the temperature and water activity of the oil of a transformer are implemented. Calculations are done on the probe data to determine the vapour pressure of the water dissolved in the oil using equation (19). The moisture concentration at the cellulose surface in contact with oil was then determined using the Fessler's equation (20), [20], [21].

$$P_v = z.A_w.e^{\frac{k_1(\theta_{cel}+273)}{a_1+\theta_{cel}+273}} \quad (19)$$

$$WCP = s.P_v^{0.6685}.e^{\frac{w}{\theta_{cel}}} \quad (20)$$

where, $s = 2.173 \times 10^{-7}$, $w = 4725.6$, $z = 6.032 \times 10^{-3}$, $k_1 = 17.502$, $a_1 = 240.97$, P_v is vapour pressure, and is dependent on cellulose temperature (θ_{cel}) and water activity (A_w) in oil. The water activity is the relative ratio of the partial pressure of moisture in cellulose and the saturation vapor pressure of pure moisture under the same temperature [20], [21].

Equations in [8], [12], [22]-[23] are used to calculate paper insulation thermal resistance as a function of temperature and insulation moisture. Using the heat transfer theory [8] and the influence of water content (moisture) at different temperatures on thermal conductivity of oil-impregnated cellulose paper insulation [23], the thermal resistance of transformer cellulose is formulated. The thermal conduction resistance of cellulose (paper) is expressed as:

$$R_{cel} = \frac{l}{A_{cel}C_2[b_2+\delta.e^{\frac{w}{\theta_{cel}}}+\gamma(\theta_{cel}-60)]} \quad (21)$$

where, A_{cel} denotes the cellulose surface area, l denotes the thickness of cellulose, $w = 4725.6$, $C_2 = 0.176$ $\gamma = 7.3 \times 10^{-4}$, $b_2 = 0.9963$, $\delta = 7.822 \times 10^{-10} \times P_v^{0.6685}$

Substituting the nonlinear thermal equations of oil and paper into equation (2), the following expression is obtained:

$$q_{Fe} + q_{Cu} + q_{Rad} = (C_{cel} + C_{oil})\frac{d\theta_o}{dt} + \frac{\theta_o - \theta_a}{\left[\left(\frac{\mu^n}{A_O.C_1\Delta\theta_O^n}+\nu\right)+\frac{l}{A_{cel}C_2[b_2+\delta.e^{\frac{w}{\theta_{cel}}}+\gamma(\theta_{cel}-60)]}\right]} \quad (22)$$

Defining the various parameters as:

$$\mu_{pu}^n = \mu^n/\mu_R^n = e^{\frac{2797.3}{\theta_o+273}}/e^{\frac{2797.3}{\theta_{o,R}+273}} \quad (23)$$

$$R_{oil,R} = \frac{\mu_R^n}{A_O.C_1\Delta\theta_{o,R}^n} + \nu \quad (24)$$

$$R_{cel,R} = \frac{l}{A_{cel}C_2[b_2+\delta.e^{\frac{w}{\theta_{cel,R}+273}}+\gamma((\theta_{cel,R}+273)-60)]} \quad (25)$$

$$r_{pu} = \frac{R_{cel}}{R_{cel,R}} \quad (26)$$

$$\tau_{oil,R} = (R_{oil,R} + R_{cel,R}).(C_{oil,R} + C_{cel,R}) \quad (27)$$

$$\Delta\theta_{o,R} = (q_{Fe,R} + q_{Cu,R} + q_{Rad,R}).(R_{oil,R} + R_{cel,R} \quad (28)$$

$$R = q_{Cu}/q_{Fe} \quad (29)$$

$$K = I/I_R \quad (30)$$

$$\eta_R = R_{cel,R}/R_{oil,R} \quad (31)$$

where, $\Delta\theta_{o,R}$ is the rated top oil temperature rise over ambient temperature, $\Delta\theta_{hs,R}$ represents rated hot spot temperature rise over top oil temperature , $\tau_{o,R}$ is the oil time constant, $R_{oil,R}$ is rated thermal resistance of oil, $R_{cel,R}$ is rated thermal resistance of cellulose, μ_{pu}^n is the ratio of oil viscosity between any temperature and rated top oil temperature, r_{pu} denotes the ratio of cellulose thermal resistance between any temperature and rated temperature, K denotes the ratio between load current and rated winding current, I denotes load current of transformer winding, I_R is the rated current of transformer winding.

Equation (22) can be rewritten as (32), which is the proposed thermal equation for calculating top oil temperatures.

$$\left[\left[\frac{K^2.R+1}{R+1}\right]+\frac{q_{Rad}}{q_{Fe}+q_{Cu}}\right].\Delta\theta_{o,R} = \tau_{o,R}.\frac{d\theta_o}{dt} + \left[\frac{(\theta_o-\theta_a)^{n+1}}{\Delta\theta_{o,R}^n}.\frac{1+\eta_R}{\mu_{pu}^n+\eta_R.r_{pu}\left[\frac{\Delta\theta_o}{\Delta\theta_{o,R}}\right]^n}\right] \quad (32)$$

To enable calculations of the TOT from the differential equation (32), the equation components are as follows:

- Constants: R, n, $\tau_{o,R}$, $\Delta\theta_{o,R}$
- Input variables: K, θ_a, q_{Rad}, θ_{cel}
- Output variable: θ_o
- Independent variable: t

The implemented top oil temperature model is illustrated using the block diagram shown in Fig. 2.

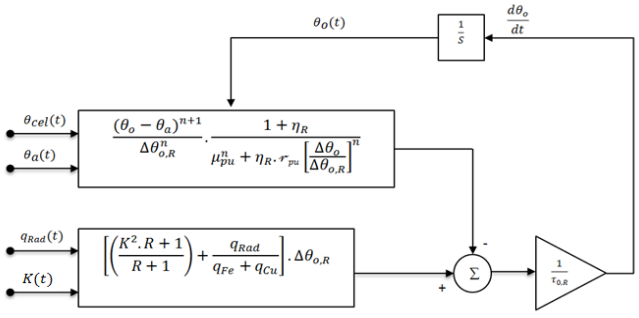

Fig 2: Block diagram of the top oil model.

2.2 Hot Spot Thermal Model

Analogous to the conventional heat transfer concept set for the top oil temperature modeling and the nonlinear thermal resistance, the hot spot temperature model thermal circuit is as in Fig. 3 where q_{Wnd} is the heat generated by winding losses.

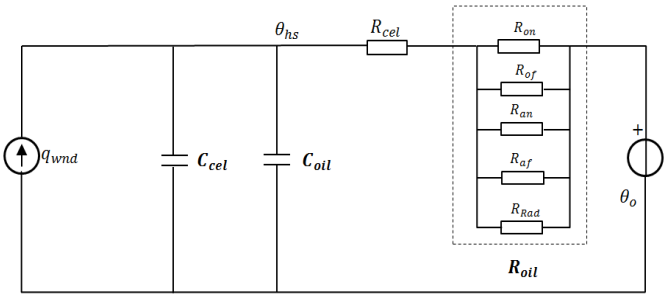

Fig 3: Hot Spot temperature thermal circuit.

From Fig. 3, the differential equation for modeling the hot spot temperature is stated as:

$$q_{Wnd} = (C_{cel} + C_{oil})\frac{d\theta_{hs}}{dt} + \frac{\theta_{hs}-\theta_o}{R_{oil}+R_{cel}} \quad (33)$$

The thermal resistance of oil and cellulose used in hot spot temperature modeling were derived in the same manner as those of top oil temperature modeling. The resulting equation for the hot spot temperature calculation is:

$$K^2 P_{Wnd,pu}.\Delta\theta_{hs,R} = \tau_{wd,R}.\frac{d\theta_{hs}}{dt}\left[\frac{(\theta_{hs}-\theta_o)^{m+1}}{\Delta\theta_{hs,R}^{m}}.\frac{1+\eta_R}{\mu_{pu}^{m}+\eta_R.r_{pu}\left[\frac{\Delta\theta_{hs}}{\Delta\theta_{hs,R}}\right]^{m}}\right] \quad (34)$$

where, $\Delta\theta_{hs,R}$ is rated hot spot temperature rise above top oil, θ_{hs} represents hot spot temperature, $\tau_{wd,R}$ denotes rated hot spot time constant, $P_{Wnd,pu}$ is the winding loss per unit, m is the nonlinearity constant for hot spot thermal model for different cooling modes.

The winding loss, which is temperature dependent, is given by:

$$P_{Wnd,pu} = P_{DC,pu}.\frac{\theta_k+\theta_{hs}}{\theta_k+\theta_{hs,R}} + P_{ED,pu}.\frac{\theta_k+\theta_{hs,R}}{\theta_k+\theta_{hs}} \quad (35)$$

where, $P_{DC,pu}$ is per unit value of DC loss, $P_{ED,pu}$ is per unit value of eddy loss, θ_k is the temperature factor for the loss correction equal to 225 for Aluminum and 234.5 for Copper.

The hot spot temperature can be determined by using equation (34) whereby the equations elements are:

- Constants: m, $\tau_{wd,R}$, $\Delta\theta_{hs,R}$, $P_{DC,pu}$, $P_{ED,pu}$
- Input variables: K, θ_{cel} , θ_o (obtained from (32))
- Output variable: θ_{hs}
- Independent variable: t

The hot spot temperature model is illustrated using the block diagram shown in Fig. 4.

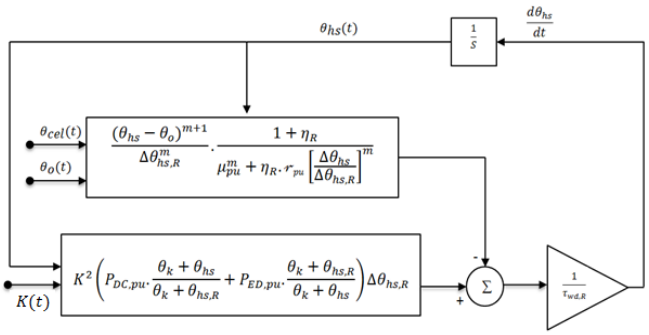

Fig 4: Block diagram of the hot spot model.

3. RESULTS AND DISCUSSIONS

The measured data set from two transformers is used for validation of the proposed thermal models. Top oil and winding temperatures (HST) were obtained from temperature indicators installed on the transformers. Model parameters were defined from the measured top oil and hot spot temperatures. Comparison of the measured top oil temperatures from in-service transformers and the model output was done. In addition, the simulated hot spot temperatures are compared with the conventional winding temperature indicator (WTI) readings. Furthermore, comparison between the proposed models with other existing thermal-electric analogy models is performed to assess the performance of the developed thermal models.

Table 1, shows the transformer characteristics for thermal modeling whilst, Table 2 shows data for solar irradiation estimations corresponding to Southern Sahara region (Africa).

Table 1: Transformer Data for TOT and HST estimation

Characteristic	Tx1	Tx2
Cooling System	ONAN/ONAF	ONAN/OFAF
Rated Power (MVA)	60/90	90/175
Rated Voltage (kV)	132/11	420/132/11
R	6.5	6.2
n	0.25	0.25
m	0.25	0.25
$\Delta\theta_{o,R}$	47.3°C	42.3°C
$\Delta\theta_{hs,R}$	20.3°C	21.8°C
$\tau_{o,R}$	108mins	115mis
$\tau_{wd,R}$	6mins	8mins
Total number of fans	10	8

Table 2: Solar irradiation estimation data, Southern Sahara Africa

Characteristic	Tx1	Tx2
Transformer Rated Power (MVA)	60/90	90/175
Average area (A_{tr}) solar irradiation contact (m^2)	12.6	18
Latitude [degrees South]	17.8	17.3
Longitude [degrees East]	30.9	31.3
GMT difference [hours]	+2	+2
Load Losses (kW)	293.9	411.72
No Load Losses (kW)	45.17	66.4
Emissivity factor (grey paint)	0.75	0.75

Fig. 5 illustrates the recorded variations in transformer load profile for Transformer 1 (Tx1) whilst, in Fig. 6 the recorded hourly ambient temperatures are presented.

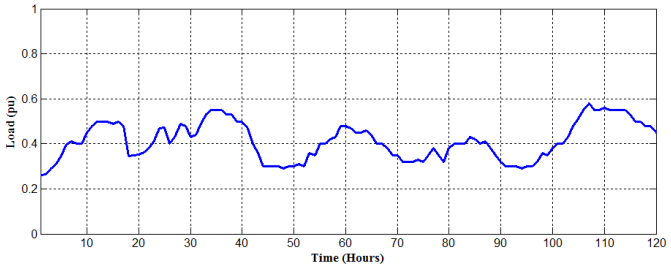

Fig 5: Transformer loadings for (Tx1).

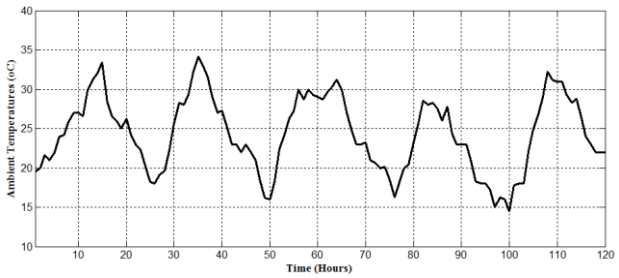

Fig 6: Ambient temperatures for (Tx1).

The cellulose temperature of an in-service transformer is normally unevenly distributed thus, in this paper, the obtained average cellulose temperatures were calculated as average of measured hot spot temperatures (θ_{hs}) and top oil temperatures (θ_o), ($\theta_{cel} = (\theta_{hs} + (\theta_o)/2$). The calculated average cellulose temperatures are highlighted in Fig. 7. Using the online moisture capacitive reading probes, the observed water activity is recorded in Fig. 8, whilst recordings of moisture concentration in cellulose of less than 1.5% is shown in Fig. 9, which indicates the transformer's cellulose is fairly dry.

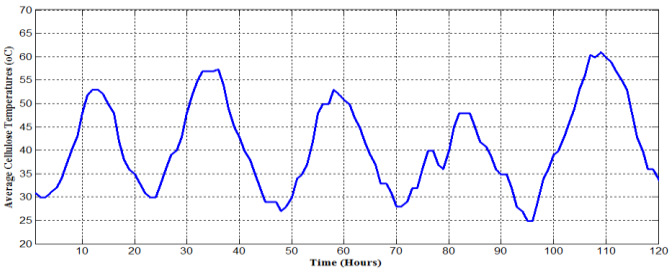

Fig 7: Average cellulose temperatures for (Tx1).

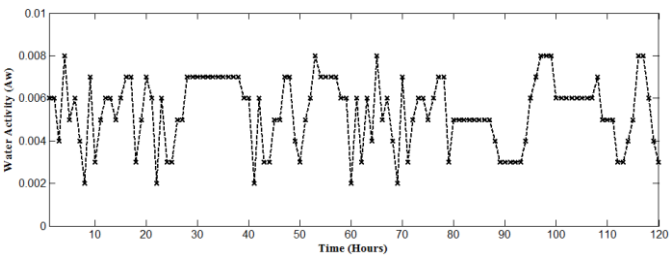

Fig 8: Water activity in cellulose insulation for (Tx1).

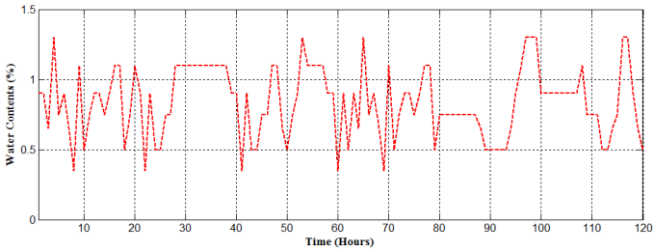

Fig 9: Cellulose moisture concentration estimation for (Tx1)

Comparisons between different thermal model outputs and onsite measurements of top oil temperatures for Transformer 1 are shown in Figs. 10. In Figures 11 the estimated hot spot temperatures by the different models inclusive of the measured hot spot temperatures are recorded. The input load used in modeling was from the middle winding phase of the transformer. Other, existing thermal-electric analogy models included in performance comparison are Swift [6], Susa [8] and Moisture-Dependent Thermal Model (MDTM) [12]. The simulated results (Fig. 10 and 11) of the proposed thermal models are in agreement with the measured values. In addition, the proposed model and MDTM were close to the measured values because they took into account the effect of moisture in calculation of nonlinear thermal resistance of transformer insulation. However, the impact of solar irradiation and improved mineral oil nonlinear thermal resistance in the proposed model improves the results compared to other models. It is also noted that other model results are underestimates highlighting the importance of including solar radiation, which has an influence in top oil temperature rise. In this paper, the thermal resistance of a transformer depends on the varying temperature whereas in most models, the thermal resistance was considered constant for every loading condition and temperature. As shown in Fig. 10 and 11, Swift's models have relatively large error in both TOT and HST estimation, which also supports observations highlighted in [12], [24].

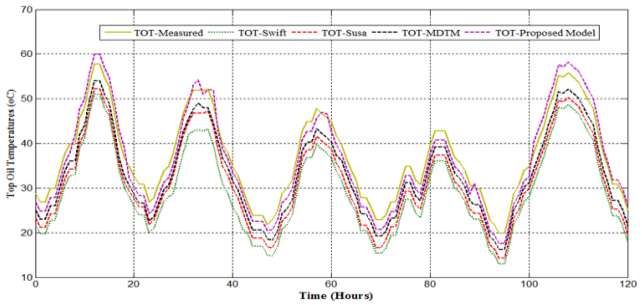

Fig. 10: Top oil temperatures for (Tx1).

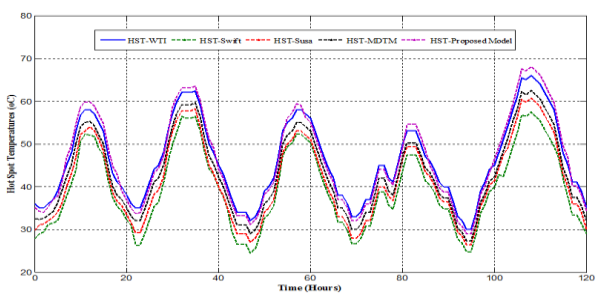

Fig. 11: Hot Spot Temperatures for (Tx1).

Performance analysis of the proposed model is done from a statistical assessment amid existing thermal-electric analogy models (Swift, Susa and Moisture- Dependent Thermal model (MDTM)) through computation of adequacy and accuracy metrics [24], [25] for the estimated hot spot temperature, with reference to onsite measurements. To measure the model adequacy, the coefficient of determination (R^2) was calculated (equation (36)), and the mean squared error (MSE) aided in determining the accuracy (equation (37)).

$$R^2 = \frac{\sum_{i=1}^{n}(\theta_i-\bar{\theta})^2-\sum_{i=1}^{n}(\theta_i-\tilde{\theta}_{(i)})^2}{\sum_{i=1}^{n}(\theta_i-\bar{\theta})^2} \quad (36)$$

$$MSE = \frac{1}{n}\sum_{i=1}^{n}(\theta_i - \tilde{\theta}_{(i)})^2 \quad (37)$$

where, θ_i and $\tilde{\theta}_{(i)}$ represent the measured and estimated hot spot temperatures, $\bar{\theta}$ denotes the mean value of the measured hot-spot temperatures, n is the sample size.

The coefficient of determination that is close to 1 denotes a desirable model adequacy. The average squares of errors between model outputs and measured results determine model accuracy. MSE approaching zero is preferred. The outcomes of the two metrics are as in Tables 3 and 4 respectively (Transformer 1).

Table 3: Adequacy Metrics of thermal models (Tx1)

R^2	Swift	Susa	MDTM	Proposed Models
TOT	0.73	0.80	0.90	0.96
HST	0.67	0.83	0.92	0.98

Table 4: Accuracy Metrics of thermal models (Tx1)

MSE	Swift	Susa	MDTM	Proposed Models
TOT	54.7	30.6	14.4	4.2
HST	43.5	22.1	8.8	1.6

In Table 3, all the models show desirable coefficient of determinant, the preeminent being the proposed multi-parameter model. This exhibits that the proposed multi-parameter based thermal model has an adequate adequacy and is proficient in estimation of top oil and hot spot temperatures. From Table 4, it can be seen that the proposed model has the least mean squared error. This also shows that this model can consistently achieve greater accuracy in estimating the transformer TOT and HST. These results suggest that the proposed thermal model can reflect the thermal activities of an oil-immersed power transformer in an appropriate fashion.

2.3 TOT and HST Results for Transformer 2

Fig. 12 presents the loading profile of Transformer 2 (Tx2) for a period of 24 hours where the maximum loading of the day was 60% of the transformer full load. In Fig. 13, the ambient and average cellulose temperatures are presented. Fig. 14 and 15 shows the estimated moisture in cellulose measurement results and it can be observed that the average moisture in cellulose is less than 1.5% signifying relatively dry cellulose insulation in the transformer.

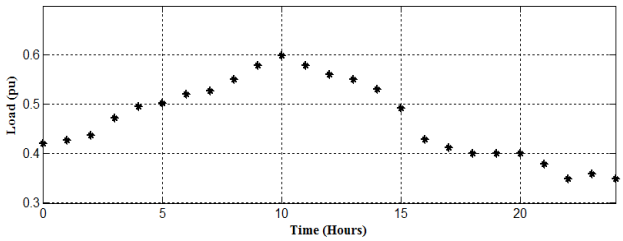

Fig. 12: Transformer loadings for (Tx2).

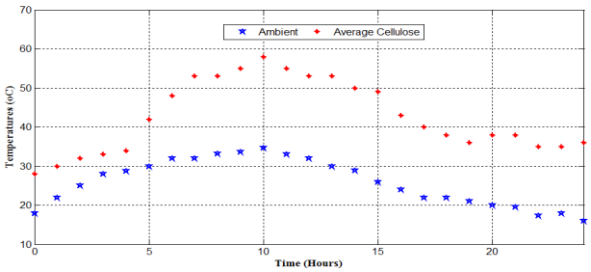

Fig. 13: Ambient and cellulose temperatures for (Tx2).

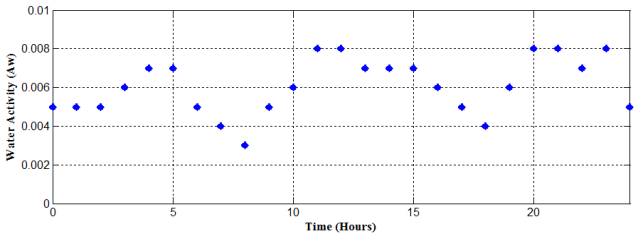

Fig. 14: Water Activity in cellulose insulation for (Tx2).

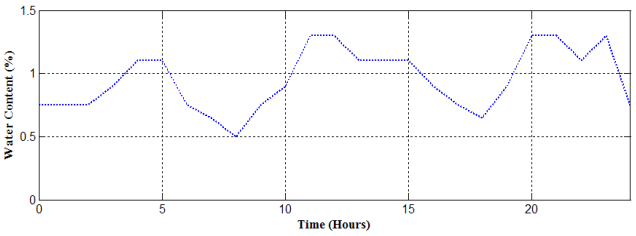

Fig. 15: Cellulose moisture concentration estimation for (Tx2)

Comparison between different thermal model outputs and on-site measurements of top oil temperatures for Transformer 2 is shown in Fig.16.

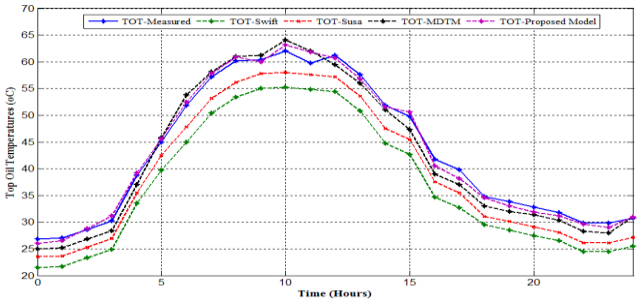

Fig.16: Top Oil Temperatures for (Tx2).

As shown in Fig. 12 and 17, when the input load current increases (not from cold start), the HST of the proposed model presents a relative smooth growth rate same as of the winding temperature indicator (WTI). The reason responsible for this rise is that the transformer oil has possesses a lower kinematic viscosity at high temperatures since the transformer was already loaded during the time of measurements. In addition, the heat flux index from solar radiation contributed positive to the top oil temperature rise which influences the HST. To control the winding temperature indicator (WTI) temperatures above 65ºC, the air forced cooling system is installed on the transformer and is automated to cater when such conditions arise. Upon time of onsite measurements, the external forced first cooling bank of fans (4 fans) were switched on at 7hours, changing ONAN to OFAF cooling mode and turned off at 13hours. Fig. 17 shows the WTI readings as compared to the developed model and the existing models. It can be seen in Fig. 17 that the proposed multi-parameter model also gives closer estimations of hot spot temperatures to the onsite measurements compared to other three models. This shows the capability of the proposed model in attaining consistent results in different transformers.

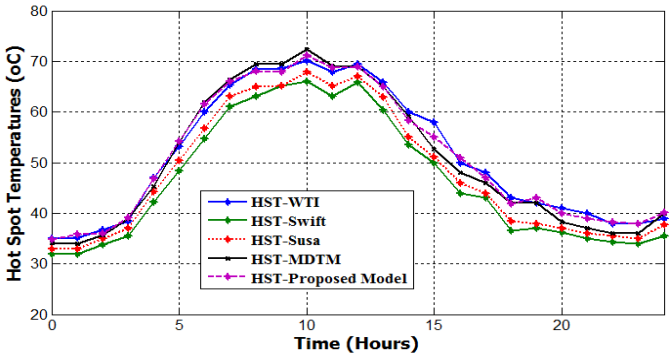

Fig 17: Hot Spot Temperatures for (Tx2).

The calculated adequacy and accuracy metrics for different thermal-electric analogy models for Transformer 2 are as shown in Tables 5 and 6, respectively. The results still indicates that the proposed model provides closer estimations of hot spot temperatures to onsite measurements than the other models.

Table 5: Adequacy Metrics of thermal models (Tx2)

R^2	Swift	Susa	MDTM	Proposed Model
TOT	0.71	0.76	0.91	0.98
HST	0.76	0.80	0.93	0.95

Table 6: Accuracy Metrics of thermal models (Tx2)

MSE	Swift	Susa	MDTM	Proposed Model
TOT	35.9	13.5	3.1	0.7
HST	22.8	11.3	3.4	1.2

4. CONCLUSIONS

Models based on thermal-electric analogy equivalent circuit for power transformer top oil and hot spot temperature are extended in this paper by including the effect of solar irradiation on thermal balance and the effect of temperature, viscosity and moisture in nonlinear resistance for oil and insulation paper (cellulose). In addition, different heat transfer modes inside the transformer are also considered. Thus, a universal model for thermal resistance for oil insulation that can be easily implemented for any transformer-cooling mode was formulated. The calculated thermal resistance was also temperature dependent. The effect of solar irradiation adds in the top oil temperature rise. Simulation results confirm that the considered parameters influence the top oil and hot spot temperature estimations. Thus, the multi-parameter based thermal model estimates the top oil and hot spot temperatures more accurately compared to the existing thermal-electric analogy models. This implies that the model approach for evaluating TOT and HST followed in this paper appears to correspond practically well with results of actual on-site measurements.

Although the proposed model gives satisfactory results on the applied transformers, the model can be further validated in transformers under heavy loading regime and in areas experiencing high solar irradiation. In addition, thermal modeling of power transformer should be inclusive of unbalanced transformer loading especially distribution transformers which are prone to spikes in loading regime. It is expected that the proposed multi-parameter based thermal model could help in transformer hot spot estimation thus, helping asset managers in cutting some costs connected with maintenance of power transformers.

5. ACKNOWLEDGEMENT

The authors gratefully acknowledge Pan African University and ZETDC for their financial support for this work to materialize. This work is an extended version of the presented manuscript in 2018 IEEE PES/IAS PowerAfrica, acknowledgement to IEEE PES/IAS PowerAfrica.

6. REFERENCES

[1]. IEEE Std C57.91-201, IEEE Guide for Loading Mineral-Oil-Immersed Transformers and Step Voltage Regulators, (Revision of IEEE Std C57.91-1995), 2012.

[2]. IEC 60076-2, Power Transformers-Temperature rise, International Electro-technical Commission (IEC) Std, 1993.

[3]. Z. Radakovic, M. Sorgic, W. Van der Veken, and G. Claessens, Ratings of oil power transformer in different cooling modes, IEEE Transactions on Power Delivery, vol. 27, no. 2, pp. 618–625, April 2012.

[4]. W. Zhan, A. E. Goulart, and P. R. Falahi, Development of a Low-cost Self-diagnostic Module for Oil-immerse Forced-Air Cooling transformers," IEEE Transactions Power Delivery, vol. 30, no.1, pp. 129–137, 2015.

[5]. J. Li, T. Jiang, and S. Grzybowski, Hot spot Temperature Models Based on Top-oil Temperature for Oil Immersed Transformers, IEEE Annual Report Conference on Electrical Insulation and Dielectric Phenomena, pp. 55-58, 2009.

[6]. G. Swift, T. S. Moliniski, and W. Lehn, A Fundamental Approach to Transformer Thermal Modeling-Part I: Theory and Equivalent Circuit, IEEE Transactions on Power Delivery, 2001, vol. 16, no. 2, pp. 171-175, 2001.

[7]. G. Swift, T. S. Moliniski, R. Bray, and R. Menzies, A Fundamental Approach to Transformer Thermal Modeling-Part II: Field Verification, IEEE Transactions on Power Delivery, vol. 16, no. 2, 2001.

[8]. D. Susa, M. Lehtonen and H. Nordman, Dynamic Thermal Modelling of Power Transformers, IEEE Transactions on Power Delivery, vol. 20, no.1, pp.197-204, 2005.

[9]. M. Djamali and S. Tenbohlen, A dynamic top oil temperature model for power transformers with consideration of the tap changer position, The 19th International Symposium on High Voltage Engineering (ISH), 2015.

[10]. S. Tenbohlen and M. Djamali, A dynamic top-oil temperature model for online assessment of overload capability of power transformers, CIGRE SC A2 COLLOQUIUM 2015 Challenges of the future for transformers & other substation equipment, September 2015.

[11]. D. Martin, Y. Cui, C. Ekanayake, H. Ma and T. Saha, An Updated Model to Determine the Life Remaining of Transformer Insulation, IEEE Transactions on Power Delivery, vol. 30, no. 1, pp.395-402, 2015.

[12]. Y. Cui, H. Ma, T. Saha, C. Ekanayake and D. Martin, Moisture-Dependent Thermal Modelling of Power Transformer, IEEE Transactions on Power Delivery, vol. 31, no. 5, pp. 2140-2150, 2016.

[13]. S. Chakravorti, D. Dey, and B. Chatterjee, Recent Trends in the Condition Monitoring of Transformers, Theory, Implementation and Analysis; Power Systems (Springer-Verlag, 2013).

[14]. Y. Cui, H. Ma and T. Saha, Transformer Hot Spot Temperature Prediction using a Hybrid Algorithm of Support Vector Regression and Information Granulation, IEEE PES Asia–Pacific Power and Energy Engineering Conference (APPEEC), pp. 1-5, 2015.

[15]. B. Gorgan, P. V. Notingher, J. M. Wetzer, H. F. A. Verhaart, P. Wouters and A.Van Schijndel, Influence of solar Irradiation on Power Transformer Thermal Balance, IEEE Transactions on Dielectrics and Electrical Insulation, vol. l9, no. 6, 2012, pp.1843-1850.

[16]. D. Y. Goswami, Principles of Solar Engineering 3rd *Edn* (CRC Press, Taylor and Francis, 2000, 42-55).

[17]. V. D. Ingenieure, VDI Heat Atlas *2nd Edn*, (Springer-Verlag Berlin Heidelberg, 2010).

[18]. M. Djamali and S. Tenbohlen, Malfunction Detection of the Cooling System in Air-Forced Power Transformers Using Online Thermal Monitoring, IEEE Transactions on Power Delivery, vol. 32, no. 2, pp. 1058-1067, 2017.

[19]. D. F. Garcia, B. Garcia, and J. Burgos, A review of moisture diffusion coefficients in transformer solid insulation—Part 1: Coefficients for paper and pressboard, IEEE Electrical Insulation Magazine, vol. 29, no. 1, pp. 46–54, 2013.

[20]. D. Martin, C. Perkasa and N. Lelekakis, Measuring paper water content of transformers: A new approach using Cellulose Isotherms in Non-equilibrium Conditions, IEEE Transactions on Power Delivery, vol. 28, no. 3, pp. 1433-1439, 2013.

[21]. D. Martin, T. Saha, O. Krause, and V. Clarkson, Improving the Online Water Content Measurement of Transformer Insulation Paper Using Low Pass Filters, IEEE Innovative Smart Grid Technologies - Asia (ISGT-Asia*)*, Nov 28-Dec 1, pp. 1043-1048, Melbourne, Australia, 2016.

[22]. D. Martin and T. Saha, A Review of the Techniques Used by Utilities to Measure the Water Content of Transformer Insulation Paper, IEEE Electrical Insulation Magazine, vol. 33, no. 3, pp. 8-16, 2017.

[23]. R. Lopatkiewicz, Z. Nadolny and P. Przybylek, The influence of water content on thermal conductivity of paper used as transformer windings insulation, Proceedings of 2012 IEEE 10th International Conference on the Properties and Applications of Dielectric Materials (ICPADMBangalore, India, pp. 1-4, July 24-28, 2012.

[24]. L. Jauregui-Rivera, and D. J. Tylavsky, Acceptability of Four Transformer Top-Oil Thermal Models-Part I: Defining Metrics, IEEE Transactions on Power Delivery, vol. 23, no. 2, pp. 1-6, 2008.

[25]. L. Jauregui-Rivera and D. J. Tylavsky, Acceptability of Four Transformer Top-Oil Thermal Models—Part II: Comparing Metrics, IEEE Transactions on Power Delivery, vol. 23, no. 2, pp.1-7, 2008.